



LAWRENCE
LIVERMORE
NATIONAL
LABORATORY

Fully Kinetic Simulations of MegaJoule-Scale Dense Plasma Focus

A. Schmidt, A. Link, D. Welch, T. Meehan, V. Tang, C.
Halvorson, M. May, E. C. Hagen

September 23, 2014

Physics of Plasmas

Disclaimer

This document was prepared as an account of work sponsored by an agency of the United States government. Neither the United States government nor Lawrence Livermore National Security, LLC, nor any of their employees makes any warranty, expressed or implied, or assumes any legal liability or responsibility for the accuracy, completeness, or usefulness of any information, apparatus, product, or process disclosed, or represents that its use would not infringe privately owned rights. Reference herein to any specific commercial product, process, or service by trade name, trademark, manufacturer, or otherwise does not necessarily constitute or imply its endorsement, recommendation, or favoring by the United States government or Lawrence Livermore National Security, LLC. The views and opinions of authors expressed herein do not necessarily state or reflect those of the United States government or Lawrence Livermore National Security, LLC, and shall not be used for advertising or product endorsement purposes.

Fully Kinetic Simulations of MegaJoule-Scale Dense Plasma Focus

A. Schmidt¹, A. Link¹, D. Welch², B. T. Meehan³, V. Tang¹, C. Halvorson¹, M. May¹, E.C. Hagen³

¹Lawrence Livermore National Laboratory, Livermore CA

²Voss Scientific, LLC, Albuquerque, NM

³National Security Technologies, LLC, Las Vegas, NV

Abstract

Dense plasma focus (DPF) Z-pinch devices are sources of copious high energy electrons and ions, x-rays, and neutrons. Megajoule-scale DPFs can generate 10^{12} neutrons per pulse in deuterium gas through a combination of thermonuclear and beam-target fusion. However, the details of the neutron production are not fully understood and past optimization efforts of these devices have been largely empirical. Previously we reported on the first fully kinetic simulations of a kilojoule-scale DPF and demonstrated that both kinetic ions and kinetic electrons are needed to reproduce experimentally observed features, such as charged-particle beam formation and anomalous resistivity. Here we present the first fully kinetic simulation of a MegaJoule DPF, with predicted ion and neutron spectra, neutron anisotropy, neutron spot size, and time history of neutron production. The total yield predicted by the simulation is in agreement with measured values, validating the kinetic model in a second energy regime.

Introduction

We describe here the first fully kinetic simulation of a MegaJoule-scale dense plasma focus (DPF) [1-4]. This simulation is appreciably more computationally intensive than kinetic modeling of kilojoule-scale devices[5, 6], due to the greater spatial scales involved and the smaller time-step needed to resolve the higher electron cyclotron frequencies associated with the higher plasma current. The neutron yield predicted by this simulation is consistent with measured neutron yields, now validating this kinetic model in a second energy/current regime.

A DPF consists of two coaxially located electrodes with a high-voltage source at one end (Figure 1). In the presence of a low-pressure gas, the high-voltage source induces a surface flashover and the formation of a current-conducting plasma sheath across an insulator at the upstream end of the DPF. During the “run-down” phase, the current sheath is accelerated down the length of the electrodes by magnetic pressure, ionizing and sweeping up neutral gas as it accelerates. When the plasma sheath reaches the end of the inner electrode, a portion is pushed radially inward during the “run-in” phase. When the leading-edge of the current sheath reaches the axis, it “pinches” the plasma to create a hot, dense region that emits high-energy electron and ion beams, x-rays, and (in the presence of D or D-T) neutrons [4].

In addition to fluid modeling, previous work has included a non-self-consistent test particle approach to access kinetic effects [7-11], kinetic simulations of a Z-pinch with scaled ion-electron mass ratio [12], and kinetic simulations of a conventional gas-puff Z-pinch [13]. We previously reported on the first fully kinetic model of a kJ-scale DPF Z-pinch device, including electrode boundaries, and demonstrated self-consistent production of high-energy charged particles and neutron production [5] as well as a detailed benchmark of the model with experiments [6].

Simulation and Experimental Set Up

The simulation set-up is briefly summarized here: calculations were performed in the particle-in-cell (PIC) code large scale plasmas (LSP) [14]. The time step was dynamically varied from 2.5×10^{-4} ns to 8×10^{-6} ns to resolve the electron cyclotron frequency. The system of Maxwell's equations on the numerical grid is solved implicitly via a matrix inversion using the PETSc linear algebra libraries [15]. The LSP algorithm, due to its energy-conserving direct implicit PIC algorithm [14], does not require spatial resolution of the Debye length to avoid numerical grid heating or temporal resolution of the plasma frequency. The calculation is initialized with density profiles, temperature profiles, and velocity profiles extracted from a 2D fluid simulation carried out using ALEGRA [16]. The fluid simulation begins with the plasma sheath at the insulator and has already begun the sheath run-in phase at 6.6 μ s, when the plasma profiles are transferred to the LSP simulation. Densities at $z < 9.5$ cm were set to 0 to reduce the total number of particles in the simulation. The kinetic simulation was then run for 11 ns prior to formation of the pinch and for an additional 15 ns of the pinch phase. The neutral gas density in front of the sheath corresponds to 3.6 torr D_2 at room temperature.

The kinetic simulation is two dimensional in cylindrical coordinates (r, z). The finest spatial resolution is in the pinch area, where cells are 100 μ m in r and 200 μ m in z . The simulated electrode geometry shown in Figure 2 corresponds to an experimental geometry used on the existing Gemini DPF in North Las Vegas. The cathodes (outer electrodes) are represented by a conducting boundary at $r = 10$ cm. In the experiment, the cathode is actually a set of 24 rectangular rods arranged in a circular pattern with gaps in between where gas can escape. The experimental anode is 57 cm long, but we model only the last 12.5 cm of it to reduce simulation run time (Figure 2).

The voltage drive is modeled with a prescribed incoming voltage wave traveling the length of the anode, with a reflected wave traveling back. The voltage is ramped up during the first 10 ns of the simulation, and then kept constant for the remainder of the simulation, resulting in a steady-state current of 1.94 MA before the pinch formation.

Simulation Results and Comparison with Experiment

The simulation was run for 26 ns, at which time it had not completely stopped producing neutrons (Figure 3). The simulation was stopped due to computing resource limitations and the remaining yield extrapolated from the simulated yield curve. Extrapolated estimates of the yield are $1.5 \cdot 2 \times 10^{11}$, which is consistent with experimentally measured yields. Figure 4 shows simulated and measured yield as a

function of current for the Gemini DPF. The measured data is taken from Be activation foil measurements from a recent experimental campaign, with current measured via Rogowski coil.

Figure 5 shows the simulated energy spectrum for D^+ ions in 0-to-10-degree forward-directed cone 5 ns after the start of pinch. The bulk of these ions have energies below 100 eV, with a high-energy tail extending to 1 MeV. Preliminary measurements of ion beam energies on the Gemini DPF using a Faraday cup time of flight (TOF) measurement have observed deuterons with energies up to 310 keV. Higher energy ions may exist but are below the signal-to-noise level of this diagnostic. Ion beams have been observed on a variety of DPFs with energies up to 8 MeV [17, 18], with higher energy ions registering 1-3 orders-of-magnitude weaker signals relative to the ~ 300 keV ions.

The simulated angular and energy distribution of the neutrons produced by the DPF is shown in Figure 6. As expected, the neutron energies are on average > 2.45 MeV, with the highest average energies occurring for neutrons traveling along the axis in the forward direction. Table 1 summarizes the simulated average neutron energies for various angles.

Angle from axis (degrees)	Average neutron energy (MeV)
0 to 20	3.09
20 to 40	3.06
40 to 60	2.90
60 to 80	2.74
80 to 110	2.57

Table 1: Simulated average neutron energy as a function of angle from axis

Figure 7 shows the simulated energy distribution of all neutrons inside and outside the $r=2.5$ mm boundary. Inside $r=2.5$ mm, the neutron production appears dominated by beam-target fusion, producing a wide spread in energies around a central peak at 2.45 MeV. Outside this region, neutrons are predominantly produced at 2.45 MeV with a ~ 11 keV width, characteristic of thermonuclear fusion or low-energy beam-target fusion.

Neutron emission as a function of distance from the axis is shown in Figure 8. The full-width half-max spot size predicted from the simulations is 1.7 mm. The neutron spot size on Gemini has not been measured, but visible camera images indicate a bright spot ~ 3 mm in diameter during the pinch.

The frequency content of simulated electromagnetic fields during the pinch is shown in Figure 9. A synthetic E_z probe was placed in the simulated plasma, 0.5 cm from the axis. The E_z field exhibits broadband fluctuations after the plasma starts pinching at 16 ns, increasing in magnitude and spectral content as the pinch lengthens. The maximum local magnetic fields are up to 400 T during the pinch, corresponding to a lower hybrid (LH) frequency of 180 GHz. The highest amplitude oscillations are all observed below 180 GHz, though oscillations of >180 GHz are observed on the probe at $<10\%$ of peak amplitude. Regions of plasma that could plausibly emit GHz radiation near this probe (where there is both a significant density and a sizable magnetic field) have magnetic fields ranging from ~ 10 -400 T, corresponding to a lower hybrid frequency range of

4.5 GHz-180 GHz. With highly non-uniform and temporally evolving magnetic fields in the simulation, the broadband oscillations observed are consistent with oscillations in the LH range of frequencies. By contrast, the range of ion cyclotron frequencies for these conditions span 0.07 to 3 GHz, while the electron cyclotron range from 0.29 to 11 THz. The spectrogram exhibits an upwards frequency chirp from 2 GHz to 10 GHz, at 19 ns to 21.5 ns, roughly corresponding to the time of maximum neutron production.

Figure 10 shows the ion density and E_z fields in the plasma at three different times, one just prior to the pinch, and two during the pinch. As the plasma implodes, Raleigh-Taylor-like fingers of plasma density form on the trailing edge of the plasma sheath. When the sheath is at maximum compression, it exhibits necking such that the smallest pinch diameter is 1 mm, while the areas with trailing mass are still as thick as 7 cm in diameter. The densest parts of the pinch are compressed up to 500 times relative to the original fill density. The E_z field forms in small pockets, mainly in the gaps between the density fingers. The E_z fields are dominantly positive, with some small areas of negative E_z as well, consistent with past DPF kinetic simulations.

Although the largest voltage drops are in low density regions at a radius of 5 mm or greater, the vast majority of the ion beam acceleration takes place in the vicinity of the high density pinch region, where there are more ions to accelerate. Here ions within 2 mm of the axis can experience a maximum integrated E_z field of 1-3 MV depending on their radius. The maximum particle energy that we observe in the simulations is 3 MeV.

In previous work we demonstrated that these kinetic simulations exhibit anomalously high plasma resistivity during the pinch [6]. In the MegaJoule-scale simulation, the plasma resistance rises to approximately 0.7 Ω at peak neutron production. This resistance (R) was obtained using the voltage between electrodes at the boundary (V), and the time-dependent current (I) and inductance (L). Resistance was solved for assuming

$$V = IR + d(LI)/dt.$$

Using a pinch length of 1 cm and a pinch radius of 2.5 mm, a plasma resistance of 0.7 Ω corresponds to a plasma resistivity of 140 m Ω -cm. A classical resistivity calculation based on local density and temperature would predict a resistivity of only 10 $\mu\Omega$ -cm in the pinch region, more than 1000x less than the observed kinetic resistivity. The anomalous plasma resistivity and fluctuations near the lower hybrid frequency in the MegaJoule-scale simulation are consistent with the classic explanation for beam formation in a pinch plasma: anomalous resistivity due to lower hybrid drift instability [19].

Summary

The simulation effort described here constitutes the first fully kinetic particle-in-cell simulation of a MJ-sized DPF, predicting neutron yields, D+ energy distribution, and angular/energy dependence of neutron production in a way that is not possible with standard fluid codes. The PIC simulation includes kinetic effects, such as ion beam formation, kinetic instabilities, and beam-target fusion. This model requires significantly increased computation time relative to the kJ-scale DPFs modeled previously due to

increased spatial scale and smaller time step needed to resolve the cyclotron frequency. Extrapolated neutron yields are in agreement with experimentally measured neutron yields for this DPF. Simulated neutron spectra from inside and outside the pinch region imply that thermonuclear or low-energy-beam-target fusion is occurring outside the pinch region and mainly beam-target fusion is occurring inside the pinch region. Anomalously high plasma resistivity, more than 1000 times classically predicted values, is observed in this simulation. The validity of the kinetic model in this new regime has important implications for optimization of these devices, which historically has been done through empirical trial-and-error due to the lack of a predictive tool.

Acknowledgements

This work performed under the auspices of the U.S. Department of Energy by Lawrence Livermore National Laboratory (LLNL) under Contract DE-AC52-07NA27344 and supported by the Laboratory Directed Research and Development Program (11-ERD-063) at LLNL. This work supported by Office of Defense Nuclear Nonproliferation Research and Development within U.S. Department of Energy's National Nuclear Security Administration. Computing support for this work came from the LLNL Institutional Computing Grand Challenge program.

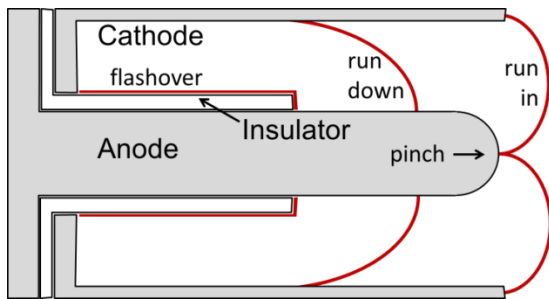


Figure 1: (Color online) Schematic of a dense plasma focus Z-pinch, including flashover, run-down, run-in, and pinch. The plasma sheath is shown in red.

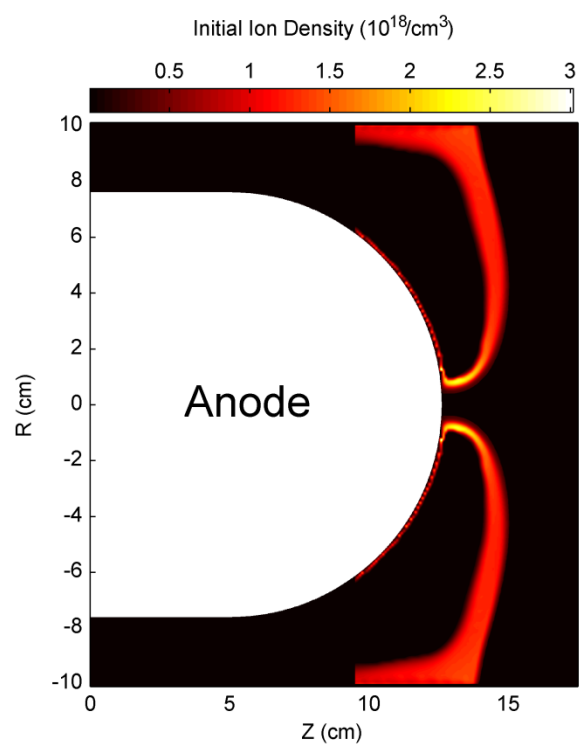


Figure 2: (Color online) Initial plasma density for kinetic simulation, as provided by a fluid simulation in ALEGRA. Densities at $z < 9.5$ cm were set to 0 to reduce the total number of particles in the simulation. In front of the sheath is neutral deuterium gas. The region behind the sheath is vacuum.

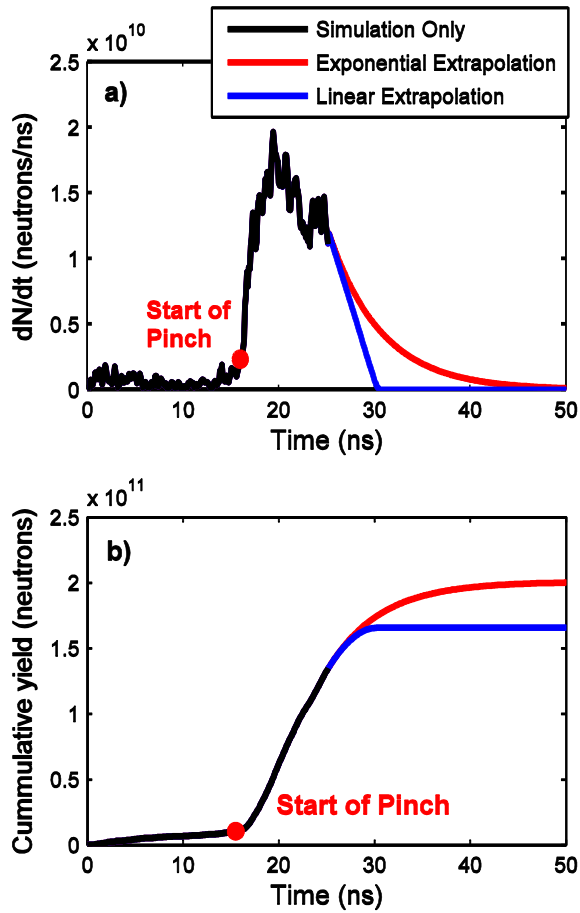


Figure 3: (Color online) (a) Neutron production as a function of time and (b) cumulative neutrons born in the simulation. Although neutron production is falling off by the time the simulation is terminated, it has not stopped completely. We use extrapolation to estimate the total predicted yield.

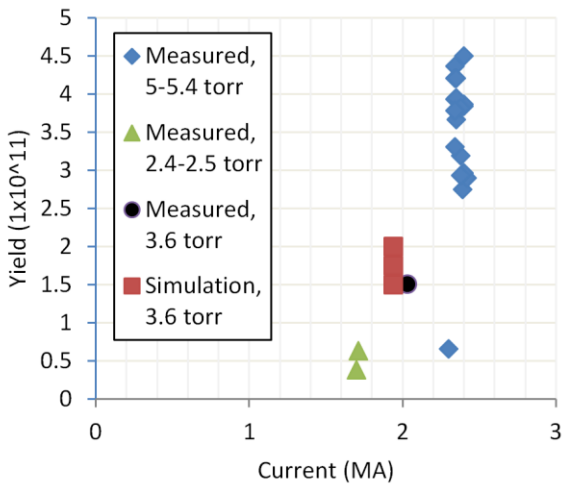


Figure 4: (Color online) Yield as a function of maximum current for the Gemini DPF, both measured experimentally and simulated. The simulation used a gas fill pressure of 3.6 torr D₂ and is closest in yield to the 3.6 torr, 2 MA shot.

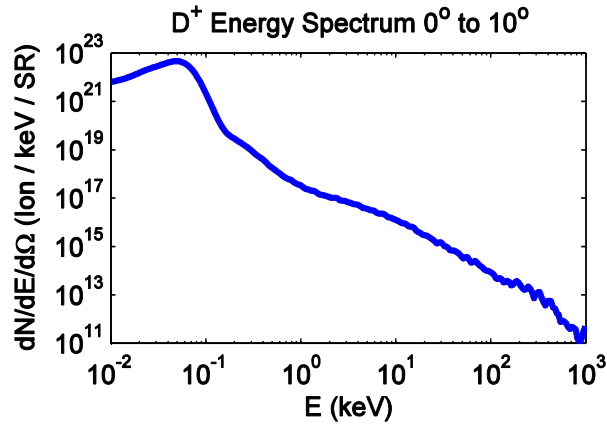


Figure 5: (Color online) Ion energy spectrum predicted by the simulation for the 0-to-10 degree velocity cone, taken from 5 ns after the start of the pinch. Above 1 MeV, the particle statistics become noisy, though we observe particles in the simulation of energies up to 3 MeV.

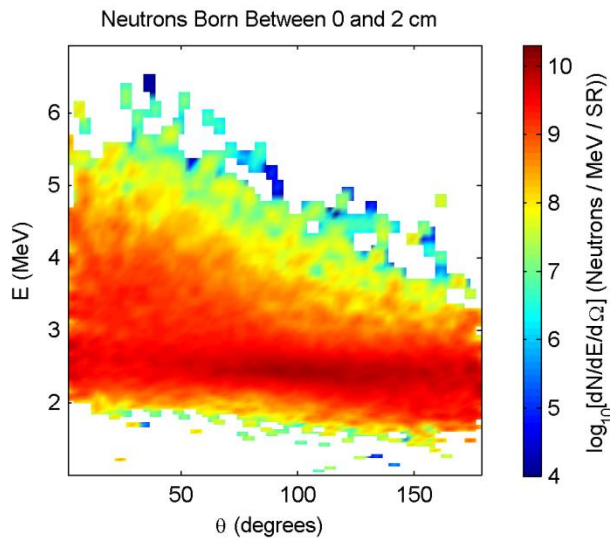


Figure 6: (Color online) Neutron production as a function of energy and angle.

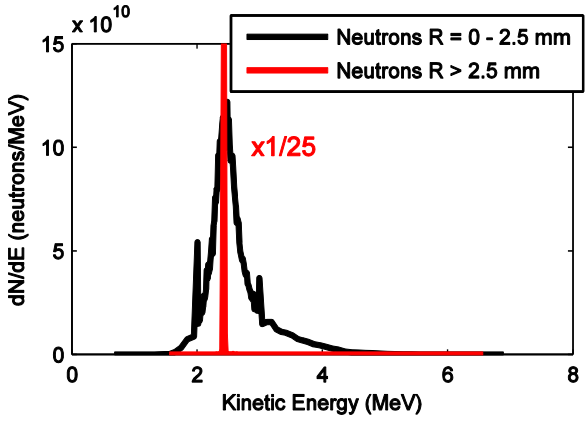


Figure 7: (Color online) Neutron energy spread inside (red) and outside (black) the pinch region. Outside the pinch region the neutron energy is sharply peaked at 2.45 MeV, with ~ 11 keV width, indicating that thermonuclear fusion or low-energy-beam-target fusion is occurring there. Inside the pinch, the energy is peaked at 2.45 MeV, but spread over a wide range of energies, mostly from 1.8 to 5.5 MeV, indicating that beam-target fusion is dominant there.

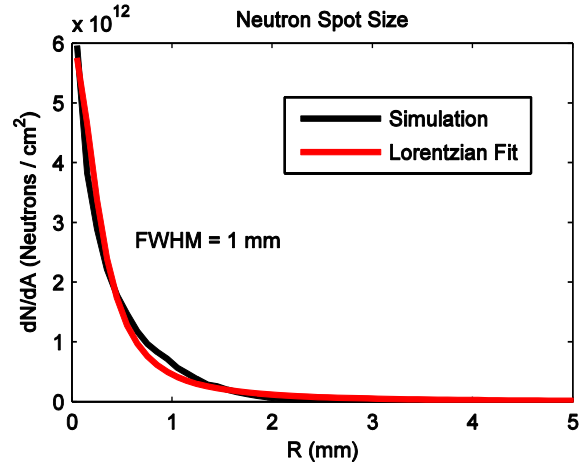


Figure 8: (Color online) Neutron emission per cross-sectional area as a function of radius.

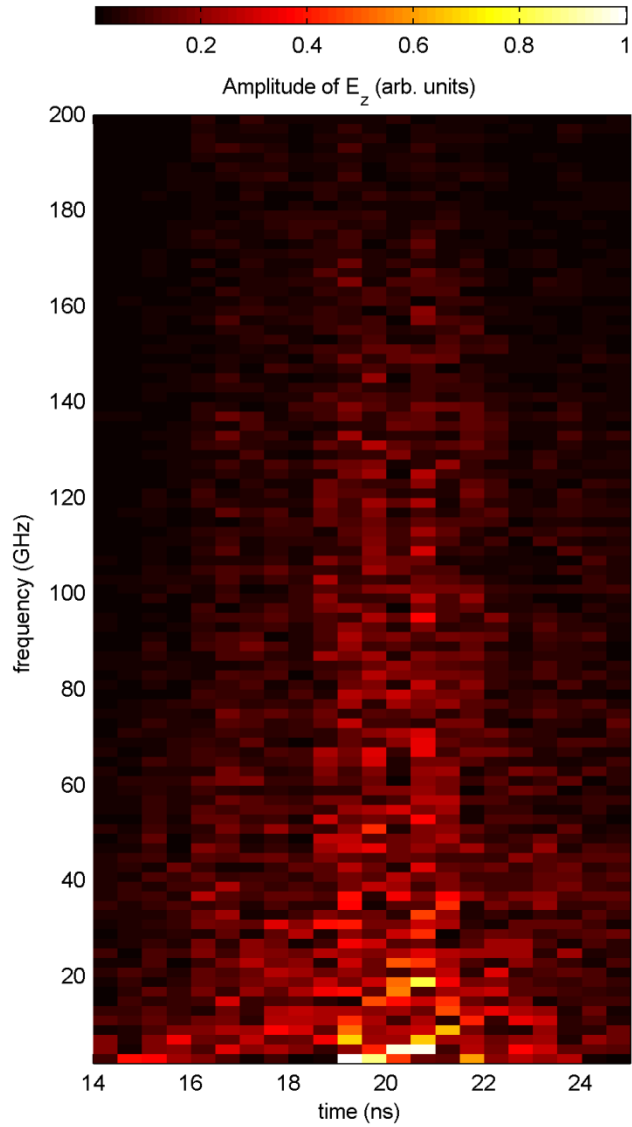


Figure 9: (Color online) Spectrogram of E_z oscillations in a simulated probe 0.5 cm in front of anode. Broadband activity begins around 15 ns and ends around 23 ns. It appears that an upwards frequency chirp is occurring from about 2 GHz to 10 GHz during 19 ns to 21.5 ns, roughly the time of maximum neutron production. Above 180 GHz, the magnitude of oscillations falls to under 10% of the maximum observed magnitude.

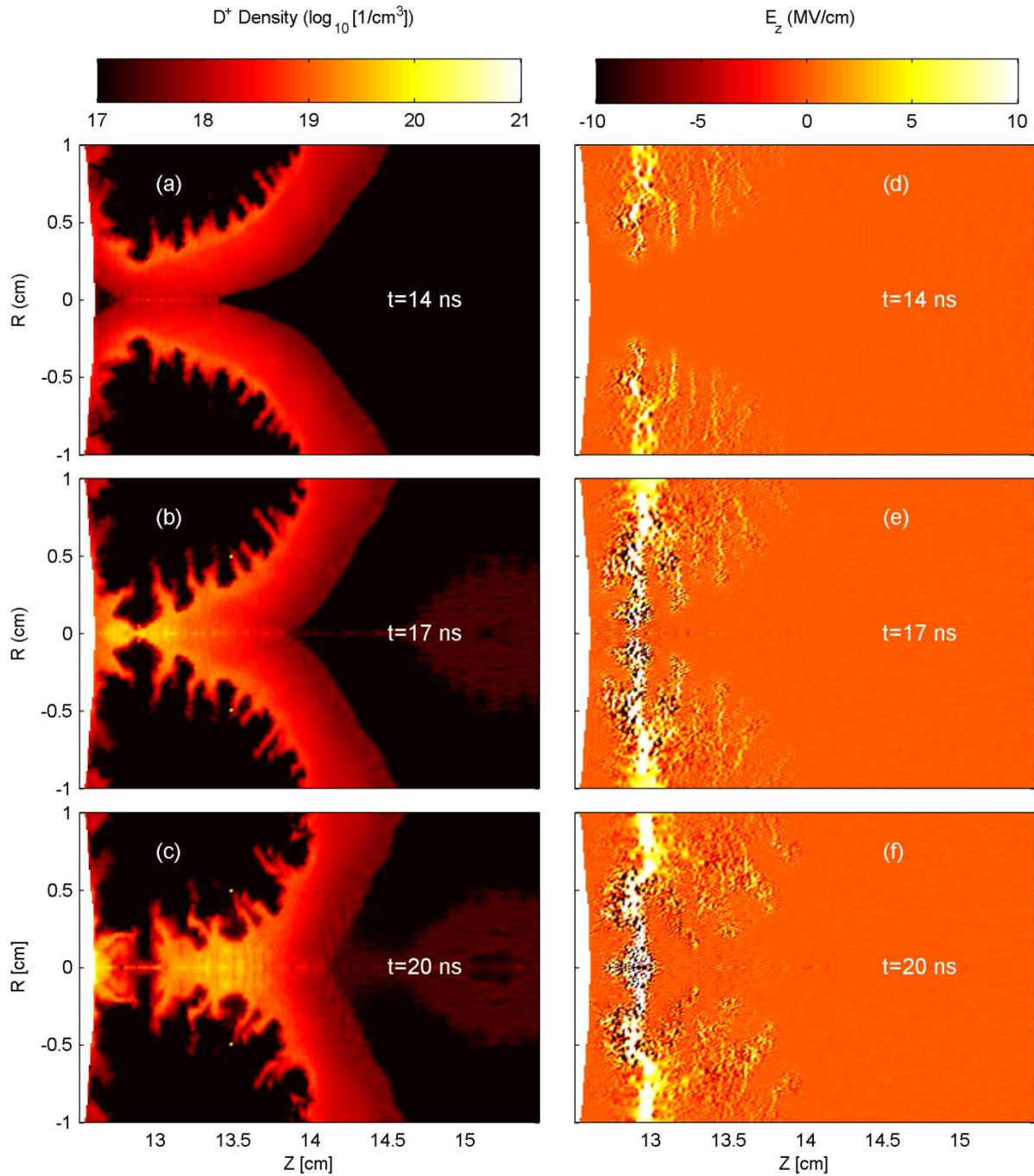


Figure 10: Ion Density and electric field in the z-direction (E_z) at 3 different times in the simulation: 14 ns (2 ns pre-pinch), 18 ns, and 21 ns. The ion density in the pinch is up to 1000 times that of the fill gas. The most dominant electric fields form in the gaps between trailing mass where there are very few particles to accelerate. Small electric field structures, on the order of 250 μm , form inside the pinch with fields as

high as 10 MV/mm. Negative E_z structures exist with the same magnitude. Integrated over the whole pinch length, E_z fields are 1-3 MV within 2 mm of the axis, depending on the radial location. The white section on the far left of each figure is the metal anode region.

1. Bernard, A., P. Cloth, H. Conrads, A. Coudeville, G. Gouylan, A. Jolas, C. Maisonnier, and J.P. Rager, *DENSE-PLASMA FOCUS - HIGH-INTENSITY NEUTRON SOURCE*. Nuclear Instruments & Methods, 1977. **145**(1): p. 191-218.
2. Haines, M.G., *A review of the dense Z-pinch*. Plasma Physics and Controlled Fusion, 2011. **53**(9): p. 093001.
3. Mather, J.W., *INVESTIGATION OF THE HIGH-ENERGY ACCELERATION MODE IN THE COAXIAL GUN*. Physics of Fluids, 1964. **7**(11): p. S28-S34.
4. Mather, J.W., *FORMATION OF A HIGH-DENSITY DEUTERIUM PLASMA FOCUS*. Physics of Fluids, 1965. **8**(2): p. 366-&.
5. Schmidt, A., V. Tang, and D. Welch, *Fully Kinetic Simulations of Dense Plasma Focus Z-Pinch Devices*. Physical Review Letters, 2012. **109**(20): p. 205003.
6. Schmidt, A., A. Link, D. Welch, J. Ellsworth, S. Falabella, and V. Tang, *Comparisons of dense-plasma-focus kinetic simulations with experimental measurements*. Physical Review E, 2014. **89**(6): p. 061101.
7. Deutsch, R., W. Kies, and G. Decker, *Theoretical-Model and Computer-Simulations of Electric Signals for Magnetically Driven Plasma Sheaths*. Plasma Physics and Controlled Fusion, 1986. **28**(12A): p. 1823-1839.
8. Gary, S.P. and F. Hohl, *Ion Kinematics in a Plasma Focus*. Physics of Fluids, 1973. **16**(7): p. 997-1002.
9. Haines, M.G., *Ion-Beam Formation in an $M = 0$ Unstable Z-Pinch*. Nuclear Instruments & Methods in Physics Research, 1983. **207**(1-2): p. 179-185.
10. Kondoh, Y. and M. Mamada, *Numerical Study on Charged-Particle Accelerations in the Plasma-Focus*. Physics of Fluids, 1986. **29**(2): p. 483-488.
11. Tang, V., M.L. Adams, and B. Rusnak, *Dense Plasma Focus Z-Pinches for High-Gradient Particle Acceleration*. IEEE Transactions on Plasma Science, 2010. **38**(4): p. 719-727.
12. Haruki, T., H.R. Yousefi, K. Masugata, J.I. Sakai, Y. Mizuguchi, N. Makino, and H. Ito, *Simulation of high-energy particle production through sausage and kink instabilities in pinched plasma discharges*. Physics of Plasmas, 2006. **13**(8): p. 082106.
13. Welch, D.R., D.V. Rose, R.E. Clark, C.B. Mostrom, W.A. Stygar, and R.J. Leeper, *Fully Kinetic Particle-in-Cell Simulations of a Deuterium Gas Puff z Pinch*. Physical Review Letters, 2009. **103**(25): p. 255002.
14. Welch, D.R., D.V. Rose, M.E. Cuneo, R.B. Campbell, and T.A. Mehlhorn, *Integrated simulation of the generation and transport of proton beams from laser-target interaction*. Physics of Plasmas, 2006. **13**(6): p. 063105.
15. Balay, S., W.D. Gropp, L.C. McInnes, and B.F. Smith, *Modern Software Tools in Scientific Computing*. 1997: Birkhäuser.
16. Allen, R., B. Thomas, C. Susan, D. Richard, G. Christopher, G. Thomas, H. Thomas, H. Heath, H. David, L. Duane, L. Raymond, L. Edward, L. Christopher, M. Stewart, N. John, O. Curtis, P. Sharon, R. William, S. Guglielmo, O. Strack, S. Randall, T. Timothy, V. Weirs, W. Michael, and V. Thomas, *ALEGRA: An Arbitrary Lagrangian-Eulerian Multimaterial, Multiphysics Code*, in *46th AIAA Aerospace Sciences Meeting and Exhibit*. 2008, American Institute of Aeronautics and Astronautics.

17. Bostick, W.H., H. Kilic, V. Nardi, and C.W. Powell, *Time-Resolved Energy-Spectrum of the Axial Ion-Beam Generated in Plasma-Focus Discharges*. Nuclear Fusion, 1993. **33**(3): p. 413-420.
18. Gullickson, R.L. and H.L. Sahlin, *Measurements of High-Energy Deuterons in Plasma-Focus Device*. Journal of Applied Physics, 1978. **49**(3): p. 1099-1105.
19. Davidson, R.C. and N.T. Gladd, *Anomalous Transport Properties Associated with Lower-Hybrid-Drift Instability*. Physics of Fluids, 1975. **18**(10): p. 1327-1335.